# Short-time solvation dynamics probed by phase-locked heterodyne detected pump-probe

de Boeij, W.P.; Pshenichnikov, M.S; Wiersma, D. A.

*Published in:*
Chemical Physics Letters

*DOI:*
10.1016/0009-2614(95)01217-6



*Publication date:*
1995

22 December 1995

ELSEVIER

Chemical Physics Letters 247 (1995) 264–270

CHEMICAL PHYSICS LETTERS

# Short-time solvation dynamics probed by phase-locked heterodyne detected pump–probe

Wim P. de Boeij, Maxim S. Pshenichnikov, Douwe A. Wiersma

*Ultrafast Laser and Spectroscopy Laboratory, Department of Chemistry, Materials Science Centre, University of Groningen, Nijenborgh 4, 9747 AG Groningen, The Netherlands*

Received 5 October 1995

**Abstract**

Phase-locked heterodyne detected pump–probe experiments are reported on solutions of a dye molecule in ethylene glycol, methanol and acetonitrile. By performing experiments at different phase-lock wavelengths, the real and imaginary parts of the line broadening function $g(t)$ could be mapped out. The imaginary part of $g(t)$ is directly related to dissipative dynamics. Comparison of the experimental data with calculations based on the Brownian oscillator model yields solvation frequencies that are substantial higher than those reported using MD simulations on similar systems.

## 1. Introduction

There is compelling evidence, both from molecular dynamics (MD) simulations [1–4] and femtosecond fluorescence upconversion experiments [5,6], that the initial phase of polar solvation dynamics proceeds on a time scale of less than 100 fs. MD simulations also revealed that this initial ultrafast solvation step is inertial; that is, it is due to small-amplitude free rotational motions of solvent molecules, with the bulk of the solvation being caused by dynamics in the first solvation shell. While this initial solvation phase is a single-molecule event, the initial conditions for these unimpeded molecular motions are, of course, being determined – as nonequilibrium MD simulations show – by all solute–solvent interactions on the ground state potential energy surface. Despite the fact that there has not been a single experiment revealing the inertial effect *directly*, its existence has been taken for granted. Yet, a direct measurement of the inertial effect would be rather important, not merely as prove of its existence, but also to confirm the validity of *classical* MD simulations for a description of solvation dynamics. Furthermore, the unveiling of the inertial effect would put to rest some questions concerning the applicability of Bloch-like models for a description of ultrafast optical dynamics in solution. Study of the short-time solvation dynamics is also important in itself as it is directly connected to chemical reactivity [7] in the solution phase and in proteins.

Experimentally solvent and solvation dynamics – as probed in time-gated fluorescence or in a variety of four-wave mixing experiments – have been modeled extensively [8–14] by use of the multimode Brownian oscillator (MBO) model [15], which is applicable to describe solvation dynamics at all times. In this model the harmonic oscillators, representing solvent motions or intramolecular vibrations, can be under- or overdamped. While purely phenomenologi-


*SSDI* 0009-2614(95)01217-6

cal, the MBO model has had an enormous impact on our thinking about optical dynamics in solution. For instance, it is now well accepted that optical dynamics in solution is distinctly non-Markovian, meaning that the bath correlation function cannot be represented by a delta function in time (Markov approximation). The attractiveness of the MBO model stems also from the fact that it makes a direct link between optical and solvation dynamics [16]. This has made the MBO model a popular formalism to describe and connect a variety of linear and nonlinear spectroscopic measurements. In MBO theory a major role is played by the so-called line broadening function $g(t)$, whose imaginary part is directly related to solvation dynamics, and which determines the nonlinear optical response functions.

We have recently shown [17] that phase-locked heterodyne detected pump–probe experiments provide direct access to the short-time behaviour of $g(t)$. Fig. 1 shows the pulse sequence for femtosecond phase-locked pump-probe (PLPP). PLPP is a pump–probe experiment in the sense that the excitation pulse pair creates a population state, which is interrogated by a third pulse. The difference with conventional pump–probe is that the state of population is an ordered state; it can be viewed as a grating in frequency space, which is affected by short-time dynamics. This is reflected in the probing process whereby the population is converted into a polarization that interferes with the third pulse. PLPP can also be viewed also as a special case of heterodyne detected stimulated photon echo [17].

For the dye DTTCI in ethylene glycol these experiments led to the conclusion that no noticeable solvation dynamics occurred in the first 50 fs. In this Letter we present some new and more detailed results of PLPP experiments on DTTCI (3,3′-diethylthiatricarbocyanine iodide), in ethylene glycol (EG), methanol (MeOH), and acetonitrile (AN) at room temperature. Sub-100 fs dynamics is deduced now in all solvents, be it that solvation is noticeably slower in EG than in AN or MeOH. It is pointed out that intramolecular vibrational dynamics contributes to the short-time dynamics of $g(t)$. Intramolecular dynamics can only be separated from solvent dynamics for vibrational modes that are prominent in the stimulated photon echo.

## 2. Experimental

The setup used to perform the fs PLPP experiments is shown in Fig. 2. It is a modified version of the apparatus employed before to conduct phase-locked heterodyne detected stimulated photon echo experiments [17]. The setup is constructed around a home-built cavity-dumped Ti:sapphire laser [18], whose spectral output peaks at 780–785 nm. The dumped laser pulses, after pre-compression in a four fused-silica prism assembly, are split by a 50%

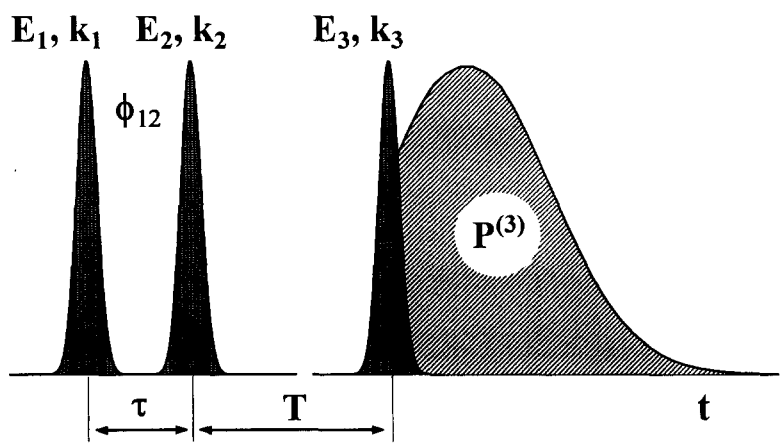


Fig. 1. Pulse sequence for phase-locked pump–probe experiments. Wavevectors of the pump fields $E_1$ and $E_2$ are equal: $\boldsymbol{k}_1 = \boldsymbol{k}_2$, while the difference between their phases $\phi_{12} = \phi_1 - \phi_2$ is fixed for any delay time $\tau$. The induced third-order polarization $P^{(3)}$ is probed at the time $t = 0$.

beamsplitter (BS1). One of the beams is directed to Mach–Zehnder interferometer (MZI) which produces a sequence of two interferometrically stable pump pulses $E_1$ and $E_2$ (Fig. 1) separated by time $\tau$. A precision translation stage in combination with a ceramic piezo transducer (PZT) enable accurate control of the delay between the pulses of a pulse pair.

Phase-locking of time-separated femtosecond laser pulses was achieved by monitoring the electric field interferences through a narrow band monochromator [19,20]. The obtained spectral interference pattern is the Fourier transform of the pulse pair and thus directly reflects the phase difference and delay between the pulses. Active control and stabilization of the phase can now be obtained by use of an appropriate feedback loop, thereby maintaining the total accumulated phase angle ($\phi = \omega_{\text{lock}}\tau$, with $\omega_{\text{lock}}$ the locking frequency and $\tau$ the delay between the pulses) at a specific value; for instance, in-phase $\phi = 2n\pi$ while for in-quadrature $\phi = (2n \pm 1/2)\pi$.

The probe pulse $E_3$, after being delayed by a time $T$, and the phase-locked pump pair were focused in the sample jet under a small angle and recollimated using all reflective optics. Dye solutions of DTTCI (Lambda Physik) in EG, AN or MeOH (Merck p.A.) were made with a peak optical density of about 0.2 over a jet thickness of 100 μm. After traversing the jet the pump pair was focused into a 30 or 100 μm BBO crystal to measure a second-harmonic phase-locked interferometric collinear autocorrelation function. It yielded a pulse duration of 13–15 fs (assuming a sech [2] pulse envelop shape), independent of whether the jet was off or on. The autocorrelation signal was recorded permanently during the PLPP experiments providing an accurate determination of zero delay within the pump pair and continuous inspection of the phase-locking process. The zero delay point between the pump pulses and the probe pulse was set by recording two-pulse photon echo signals in conjugated directions.

The PLPP signal was detected by a silicon photodiode (PD1) positioned in the beam carrying the probe pulse, and processed by a lock-in amplifier. It was referenced to the sum-frequency of a dual-frequency mechanical chopper that modulates both pump beams. In this manner we select contributions to the signal that result only from an interaction with all laser fields. Excitation pulse energies were kept as low as 250 pJ per pulse to avoid interference with higher-order (for instance, $\chi^{(5)}$) optical nonlinearities. The experiments were performed at a repetition rate of 4 MHz; lowering this rate had no effect on the signal shape. In all experiments reported here the probe delay time, $T$, was set at 5 ps, which is much longer than the decay of the vibrational coherence in DTTCI.

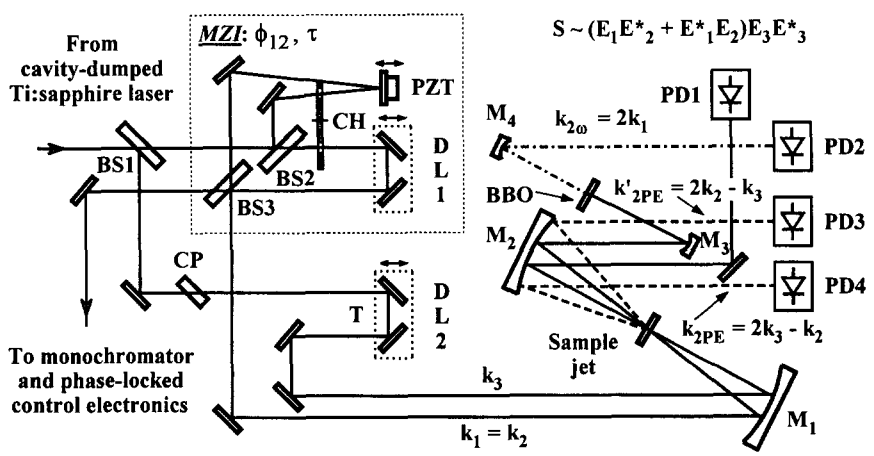


Fig. 2. Layout of the experimental setup. MZI: Mach–Zehnder interferometer, CH: dual-frequency mechanical chopper, DL: delay line, PZT: piezo-electric transducer, BS: $R = 50\%$ beamsplitter, CP: compensation plate to equalize the amount of material in each beam, M: focusing ($r = 25$ cm) mirror, BBO: 30 or 100 μm doubling crystal, PD: silicon photodiode. PD1 detects the phase-locked pump–probe signal, while PD2 monitors the phase-locked interferometric autocorrelation function. The two-pulse echo signals in conjugate directions $k_{2PE}$ and $k'_{2PE}$ (dashed lines) and detected by PD3 and PD4.

## 3. Results and discussion

Fig. 3 displays pump–probe signals with and without phase-locking for DTTCI in EG and they are found to be strikingly different. Without phase-locking (Fig. 3a) a rather 'noisy' interference pattern is observed. In the phase-locked case (Fig. 3b) – which intercepts the interference pattern at specific phase differences – the signals are very much dependent on the phase difference locked to. While the in-phase ($\phi_{12} = 0$) PLPP signal is symmetric, the in-quadrature ($\phi_{12} = \pi/2$) component of the signal is anti-symmetric. Fig. 4 shows (solid circles) how the PLPP signals vary as a function of lock-frequency. Notable differences are observed in the shape of the signals for the various solvents, especially for the in-quadrature parts near the lock-wavelength where phase reversal of the signal occurs. As will be shown these lock-wavelength-dependent changes are essential to pinpointing the short-time solvation dynamics.

In order to obtain a more quantitative analysis of the data in Fig. 4 we employ the MBO model and use results of a recent paper [17]. In that paper we showed that for impulsive excitation and positive delay time $\tau$, the PLPP signal has the following phase and delay dependence,

$$S_{\mathrm{PLPP}}(\tau,\ \phi_{12}=0) = \exp\{-\mathrm{Re}[\,g(\tau)]\} \times\cos\{\mathrm{Im}[\,g(\tau)-(\omega_{\mathrm{eg}}-\omega_{\mathrm{lock}})\tau]\},$$

$$S_{\mathrm{PLPP}}(\tau,\ \phi_{12}=\tfrac{1}{2}\pi) = \exp\{-\mathrm{Re}[\,g(\tau)]\} \times\sin\{\mathrm{Im}[\,g(\tau)-(\omega_{\mathrm{eg}}-\omega_{\mathrm{lock}})\tau]\}. \quad (1)$$

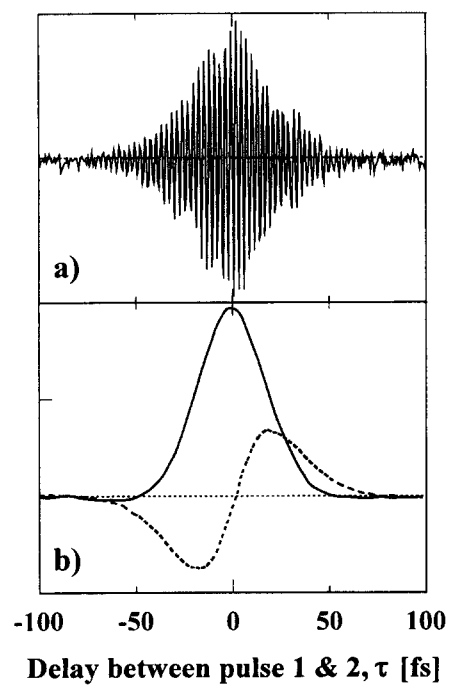


Fig. 3. Pump–probe signals without (a) and with (b) phase-locking for $\phi_{12} = 0$ (thick solid line) and $\phi_{12} = \pi/2$ (dashed line); the lock-wavelength was set at 767 nm.

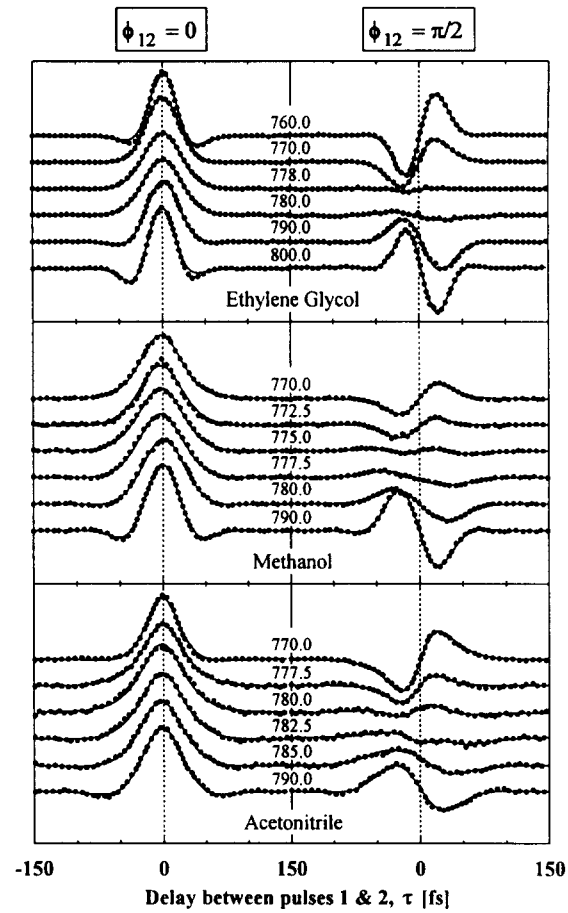


Fig. 4. Phase-locked pump–probe signals for DTTCI in the solvents ethylene glycol, methanol and acetonitrile. Lock-wavelengths (in nm) are indicated in the central part of the figure. The experimental data is represented by circles; the solid lines are the results of the computer simulations. Fit parameters are given in Table 1.

In Eq. (1), $\omega_{eg}$ is defined as the first moment of the optical absorption spectrum [21] while $\omega_{lock}$ is the lock frequency. For negative delays, $\tau$ in Eq. (1) should be replaced by $-\tau$ and the sin function preceded by a minus sign. From these considerations it is then immediately obvious why the in-phase and in-quadrature PLPP signals are symmetric and antisymmetric with respect to the delay time $\tau$.

In the MBO model the so-called line broadening function $g(t)$ in Eq. (1) can be related to the Brownian oscillator correlation function $M(t)$ as follows [15,21]

$$g(t) = -i\lambda t + i\lambda \int_0^t d\tau\, M(\tau) + \Delta^2 \int_0^t d\tau_1 \int_0^{\tau_1} d\tau_2\, M(\tau_2). \quad (2)$$

Here $\lambda$ is half the Stokes shift and $\Delta^2 = \Sigma\, \Delta_j^2$, where $\Delta_j$ is related to the frequency $\omega_j$ and displacement $d_j$ of the $j$th Brownian oscillator by the relation $\Delta_j^2 = \omega_j^2 d_j^2 [n(\omega) + \frac{1}{2}]$. $n(\omega)$ is the thermal occupation number. It should be noted that in linear response theory $M(t)$ is identical to the solvation correlation function.

For a constant $M(t)$ at short times, Eqs. (1) and (2) predict the imaginary part of $g(t)$ to be zero, resulting in a disappearance of the in-quadrature PLPP signal for $\omega_{eg} = \omega_{lock}$. Moreover, Eq. (1) predicts also the phase of the in-quadrature PLPP signal to reverse when locking above and below $\omega_{eg}$. Fig. 4 shows that for DTTCI in EG the in-quadrature PLPP signal nearly vanishes when the lock-wavelength is set to 780 nm, while the signals with lock-wavelength above and below this point have opposite phases. According to Eq. (1) then, $\lambda_{eg}$ is about 780 nm, which is redshifted from the dye's absorption maximum at 767 nm. For MeOH and AN the wavelengths at which phase reversal of the signal occurs are 775 and 785 nm, respectively. Again $\lambda_{eg}$ is above the absorption maximum. The reason for this behaviour is twofold. First, the excitation pulses have a finite spectral width and are detuned to the red with respect to the maximum of dye's absorption spectrum. Second, the absorption spectrum has an appreciable inhomogeneous component, as was inferred from time-gated photon echo experiments [22]. These facts together imply that for the analysis of our data the *effective* $\omega_{eg}$ needs to be determined. While for impulsive excitation a PLPP measurement at a single lock-wavelength is sufficient to calculate the short-time dynamics of $g(t)$, for finite excitation pulse widths a lock-wavelength-dependent study is necessary to locate $\omega_{eg}$, which is an important parameter in the analysis of the imaginary part of $g(t)$.

Inspection of Eq. (2) shows that in case $M(t)$ exhibits dynamics in the time window of our measurements (75 fs for EG, and 90 fs for AN and MeOH), Im[$g(t)$] cannot be made to vanish at *any* lock-wavelength. Qualitatively we thus conclude from Fig. 4 that solvation dynamics in AN and MeOH is much faster than in EG, which is, of course, not unexpected. To obtain a more quantitative assessment of these dynamics we tried to fit our data with a correlation function of the form

$$M(t) = \exp\left(-\tfrac{1}{2}\omega_s^2 t^2\right). \quad (3)$$

Note that $M(t)$ in Eq. (3) has the same short-time behaviour as any Brownian oscillator. $\omega_s$ is usually denoted as the solvation frequency.

In the simulations $\Delta$, $\omega_s$, and $\omega_{eg}$ were used as global fit parameters. With this set of parameters a fit was made of all in-phase and in-quadrature lock-wavelength-dependent PLPP signals. The parameter $\lambda$ was calculated from $\Delta$ and $\omega_s$, taking into account the thermally averaged occupation number of the oscillator at room temperature. In the simulations small phase errors of a few degrees were allowed for to mimic the observed asymmetry in some PLPP signals. The PLPP signals, although measured at different lock-wavelengths, were fitted with a *single* global amplitude parameter.

As was shown in our earlier papers a worthwhile analysis of fs echo type experiments must include the effect of finite pulse duration. In this Letter this effect was taken into account by employing an experimental response function of 20 fs width, being the electric field width of the optical light field. For DTTCI in EG it was verified that this approach gave very similar results compared to the much more lengthy calculations which included the finite pulse width. Table 1 provides a list of the fit parameters used in the simulation of the data displayed in Fig. 4. The solvation frequencies obtained from some MD simulations [23,24] are also included in this table. The PLPP signals calculated using the convolution

approach are depicted by the solid lines in Fig. 4. The fits are clearly excellent, reproducing as well the more subtle details of the signal shapes, above and below $\omega_{eg}$. The quality of the fits obtained implies also that a more elaborate correlation function then presented by Eq. (3) is not warranted. For instance, we have also made simulations by adding a constant term to $M(t)$, representing slower solvent motions, however a global fit of the data to this bimodal correlation function leads to a negligible weight of the constant term. This implies that PLPP does not seem to be sensitive to slow solvent motions. These latter motions are clearly evident in stimulated photon echo shift measurements. Fig. 5 presents the correlation functions (a), and imaginary (b) and real (c) parts of $g(t)$ obtained from fitting the data in Fig. 4. Note that unlike our previous, preliminary analysis, in EG there is solvation dynamics on a fast time scale, be it much less pronounced than for MeOH and AN.

Prior to commenting on the fit parameters we point out that our analysis has not yet included the effect of possible intramolecular vibrations on the short-time dynamics of $g(t)$. Frequency-resolved pump–probe and stimulated photon echo measurements exhibit quantum beats, clearly signalling the importance of this effect to the analysis of PLPP. From these measurements vibrational modes of 156, 383 and 492 $cm^{-1}$ were derived. In all solvents the 156 $cm^{-1}$ mode dominates in the quantum beat pattern. Furthermore the decay of this vibrational mode in all solvents occurs on the same time scale (about 600 fs), which is long compared to the short-time dynamics discussed here.

It is easy to show that intramolecular vibrational modes contribute to the short-time dynamics of $g(t)$ in a similar fashion as ultrafast solute–solvent dynamics. The reasoning goes as follows. In the MBO model, a vibrational mode is dealt with as a damped harmonic oscillator. Its short-time correlation function can be written as: $M(t) = 1 - \frac{1}{2}\omega_v^2 t^2$, which is identical to the limiting behaviour of $M(t)$ in Eq. (3). For the 156 $cm^{-1}$ vibrational mode this corresponds to a 'solvation' frequency ($\omega_v$) of 29 THz, which is of similar magnitude as the solvation frequencies extracted from our PLPP experiments. Thus, clearly we cannot ignore the contribution of intramolecular vibrational dynamics to the short-time dynamics of $g(t)$. This makes physical sense also because both intramolecular vibrational as well as solvation dynamics contribute to the observed Stokes shift in emission. In fact it has been suggested [13] that the Stokes shift in cyanine dyes is dominated by intramolecular vibrational relaxation. For DTTCI in EG an MBO analysis of conventional frequency-resolved pump–probe measurements yields that about 20% of the Stokes shift is caused by vibrational relaxation effects [25]. Then, how can separate sol-

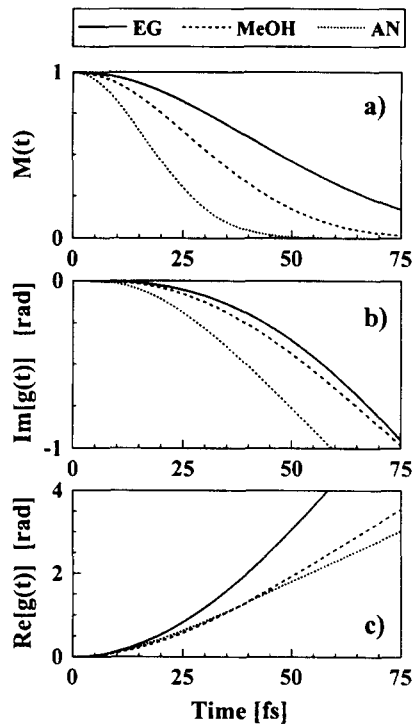


Fig. 5. Correlation function (a), imaginary (b) and real (c) parts of the line-shape function, as derived from the fits shown in Fig. 4, for ethylene glycol, methanol and acetonitrile.

Table 1
Fitting parameters

| Solvent | $\Delta$ (THz) | $\lambda$ (THz) | $\omega_s$ (THz) | | $\lambda_{eg}$ (nm) |
|---|---|---|---|---|---|
| | | | fit | MD [a] | |
| EG | 52.6 | 34.1 | 25 | – | 779.7 |
| MeOH | 44.5 | 23.5 | 38 | ≈ 25 [23] | 776.3 |
| AN | 49.1 | 25.6 | 62 | ≈ 10 [24] | 784.2 |

[a] Solvation frequencies as obtained from molecular dynamics simulations on the solute coumarin 153.

vent from intramolecular dynamics in PLPP? As stated above, the vibrational dynamics are very similar in all solvents, yet, as Fig. 4 indicates, the PLPP signals differ markedly. It is quite clear then that there must be a sizeable solute–solvent component in the ultrafast optical dynamics of DTTCI in MeOH and AN.

At this moment we do not want to enter into a discussion of how to separate the intramolecular from the solute–solvent contribution to the measured solvation frequencies. The obtained solvation frequencies are therefore lower limits of the 'true' solvation frequencies determined by solute–solvent coupling only. The only firm conclusion we can draw is that in all solvents there is an ultrafast, non-Markovian, dynamical process on a time scale of less than 100 fs. However, whatever the cause of the ultrafast response is, it cannot be determined entirely by the prominent vibrational modes and it is much faster than predicted by molecular dynamics simulations.

Summarizing, we have reported and discussed phase-locked pump–probe experiments on a dye molecule in different solvents. The real and imaginary parts of $g(t)$ were separated and fit with a Gaussian correlation function. The initial decay of this correlation function is found to be extremely fast in all solvents, manifesting itself in fs photon echo experiments as a non-Markovian dynamical process. Whether we can capture these dynamics in the realm of the multimode Brownian oscillator model is not clear yet. We are currently exploring time-gated stimulated photon echo experiments to suppress the effect of intramolecular vibrational dynamics on the decay of the echo effect. In this fashion we hope to disentangle the intramolecular from the solvent dynamical effects.

## Acknowledgement

We thank F. de Haan for providing us with software for efficient data-collection and handling. The investigations were supported by the Netherlands Foundation for Chemical Research (SON) and Physical Research (FOM) with financial aid from the Netherlands Organization for the Advancement of Science (NWO).

## References

[1] M. Maroncelli, J. Chem. Phys. 94 (1991) 2084.
[2] L. Perera and M.L. Berkowitz, J. Chem. Phys. 96 (1992) 3092; 97 (1992) 5253.
[3] E. Neria and A. Nitzan, J. Chem. Phys. 96 (1992) 5433.
[4] E.A. Carter and J.T. Hynes, J. Chem. Phys. 94 (1991) 5961.
[5] M. Cho, S.J. Rosenthal, N.F. Scherer, L.D. Ziegler and G.R. and Fleming, J. Chem. Phys. 96 (1992) 5033.
[6] R. Jimenez, G.R. Fleming, P.V. Kumar and M. Maroncelli, Nature 369 (1994) 471.
[7] P.F. Barbara, G.C. Walker and T.P. Smith, Science 256 (1992) 975.
[8] E.T.J. Nibbering, K. Duppen and D.A. Wiersma, J. Photochem. Photobiol. A 62 (1992) 347.
[9] T. Joo and A.C. Albrecht, Chem. Phys. 176 (1993) 233.
[10] K. Duppen, E.T.J. Nibbering and D.A. Wiersma, in: Proceedings of the Colloquium Femtosecond Reaction Dynamics, ed. D.A. Wiersma (North-Holland, Amsterdam, 1994) pp. 197–208.
[11] W.P. de Boeij, M.S. Pshenichnikov, K. Duppen and D.A. Wiersma, Chem. Phys. Letters 224 (1994) 243.
[12] C.J. Bardeen and C.V. Shank, Chem. Phys. Letters 226 (1994) 310.
[13] P. Vöhringer, D.C. Arnett, R.A. Westervelt, M.J. Feldstein and N.F. Scherer, J. Chem. Phys. 102 (1995) 4027.
[14] T. Joo, Y. Jia and G.R. Fleming, J. Chem. Phys. 102, 4063 (1995).
[15] Y.J. Yan and S. Mukamel, J. Chem. Phys. 89 (1988) 5160; Phys. Rev. A 41 (1990) 6485.
[16] Y.J. Yan, M. Sparpaglione and S. Mukamel, J. Phys. Chem. 92 (1988) 4842.
[17] W.P. de Boeij, M.S. Pshenichnikov and D.A. Wiersma, Chem. Phys. Letters 238 (1995) 1.
[18] M.S. Pshenichnikov, W.P. de Boeij and D.A. Wiersma, Opt. Letters 19 (1994) 572.
[19] N.F. Scherer, A.J. Ruggiero, M. Du and G.R. Fleming, J. Chem. Phys. 93 (1990) 856.
[20] N.F. Scherer, R.J. Carlson, A. Matro, M. Du, A.J. Ruggiero, V. Romero-Rochin, J.A. Cina and G.R. Fleming, J. Chem. Phys. 95 (1991) 1487.
[21] Y. Tanimura and S. Mukamel, Phys. Rev. E 47 (1993) 118.
[22] M.S. Pshenichnikov, K. Duppen and D.A. Wiersma, Phys. Rev. Letters 74 (1995) 674.
[23] S.J. Rosenthal, R. Jimenez, G.R. Fleming, P.V. Kumar and M. Maroncelli, J. Mol. Liq. 60 (1994) 25.
[24] P.V. Kumar and M. Maroncelli, J. Chem. Phys. 103 (1995) 3038.
[25] M. Emde, S. Levine, M.S. Pshenichnikov and D.A. Wiersma, unpublished result.